

Evolution of initially localized perturbations in stratified ionized disks

Edward Liverts[?] and Michael Mond

Department of Mechanical Engineering, Ben-Gurion University of the Negev,
P.O. Box 653, Beer-Sheva 84105, Israel

Accepted | . Received | -; in original form | -

ABSTRACT

A detailed solution of an initial value problem of a vertically localized initial perturbation in rotating magnetized vertically stratified disk is presented. The appropriate linearized MHD equations are solved by employing the WKB approximation and the results are verified numerically. The eigenfrequencies as well as eigenfunctions are explicitly obtained. It is demonstrated that the initial perturbation remains confined within the disk. It is further shown that thin enough disks are stable but as their thickness grows increasing number of unstable modes participate in the solution of the initial value problem. However it is demonstrated that due to the localization of the initial perturbation the growth time of the instability is significantly longer than the calculated inverse growth rate of the individual unstable eigenfunctions.

Key words: accretion, accretion discs, MHD, MRI, WKB solution.

1 INTRODUCTION

Magnetohydrodynamic (MHD) instabilities play a major role in a great variety of astrophysical and space applications. Their importance is epitomized by the magneto-rotational instability (MRI) that has been discovered by Velikhov (1959) and Chandrasekhar (1960) for finite cylinders and rediscovered by Balbus & Hawley (1991) in astrophysical context. It is widely believed to be one of the prime candidates to provide a viable clue to solving the age old puzzle of the outwards transfer of angular momentum in a plethora of astrophysical disk configurations.

However, for a case of finite size system, the common practice in stability analysis to expand the state vector of the linearized dynamical system (the MHD system of equations in our case) in plane waves as: $u(z;t) = A e^{i(\omega t + k z)}$, where z is the spatial coordinate (for simplicity only one spatial coordinate will be considered), k is the wave number, and ω is the natural frequency of the system, is not applicable especially for inhomogeneous systems. Instead, for such cases the appropriate boundary value problem (BVP) for a given set of initial conditions (IC) should be solved (see for example the well-known work of Landau (1946)). The solution of such problems is facilitated by obtaining the natural frequencies of the bounded system ω_n for which the state vector of the linearized dynamical system may be written as $u_n(z;t) = A_n(z) e^{i \omega_n t}$, where $A_n(z)$ are the eigenfunctions of the BVP subjected to specific boundary conditions (BC) (see also Sano & Miyama (1999); Coppi & Coppi (2001); Coppi & Keyes (2003)). The main purpose of the current work is to employ such approach in order to investigate the dynamical evolution of localized initial perturbations in rotating magnetized disks of finite thickness.

In reality, small perturbations, especially in a system of finite dimensions, do not have the form of a single monochromatic wave, but are rather a superposition of individual waves, i.e., wave packets. Furthermore, the asymptotic behavior at large times of the wave packet may significantly differ from that of any one of its individual components. Thus, under certain circumstances, even though some of the components of the wave packet may individually grow with time without bound, the wave packet as a whole can remain bounded at a given place and even decay to zero as the packet is convected away. In such cases the initial perturbations give rise to what is defined as convective instabilities. In other cases, the exponentially growing components of the wave packets may indeed cause the perturbation to grow without bound at each place. In such cases, the perturbations are defined as absolute instabilities. Furthermore, the BC could significantly change the results of the stability

[?] E-mail: eliverts@bgu.ac.il (EL); mond@bgu.ac.il (MM)

analysis (global stability). It is therefore of utmost importance to investigate the asymptotic (in time) development of the solutions of the appropriate Cauchy problems in order to determine whether the system is stable or not.

Various sets of rules in order to distinguish between convective and absolute instabilities have been given by Landau & Lifshitz (1959); Sturrock (1958); Fainberg et al. (1961); Akhiezer & Polovin (1971); Lifshitz & Pitaevskii (1981); Razin (2002), while Huerre & Monkevit (1990) have reviewed more recent developments of the theory pertaining to hydrodynamic stability. The importance of studying the influence of a finite system size on stability analysis has been demonstrated by Budker (1956); Sturrock (1958) who reported that the size of system could play a stabilizing role for the two stream instability.

One should note also that such understanding may play an important role in recent attempts to observe the MRI in the laboratory (Noguchi et al. 2002; Rudiger et al. 2006; Jiet al. 2006).

2 THE MAGNETOROTATIONAL INSTABILITY

2.1 Formulation of the problem and formal solution

The effect of the finite size of the system is investigated by re-examining the MRI for the case of rotating disks with finite thickness. The basic MHD equations that describe the dynamical development of the system are:

$$\frac{d\mathbf{V}}{dt} = \mathbf{f}P + \frac{1}{c}\mathbf{J} \times \mathbf{B} + \mathbf{G}; \quad \mathbf{f} \cdot \nabla = 0; \quad (1)$$

$$\frac{\partial \mathbf{B}}{\partial t} = \alpha \times \mathbf{E}; \quad \mathbf{f} \cdot \mathbf{B} = \frac{4}{c}\mathbf{J}; \quad \mathbf{f} \cdot \mathbf{B} = 0; \quad (2)$$

where \mathbf{G} is acceleration due to gravity, and c is speed of light and the rest of the variables have their usual meanings. The expression for electric field \mathbf{E} in ideal plasma is given by:

$$\mathbf{E} = -\frac{1}{c}\nabla \times \mathbf{B}; \quad (3)$$

In order to simplify the calculations (and with no loss of generality of the results) we assume that the Brunt-Vaisala frequency is small in comparison to all other characteristic frequencies in the system and can hence be neglected. Thus, the linearized MHD system of equations that describe radially independent perturbations in a Keplerian disk under the influence of a constant axial magnetic field, may be represented in the following way:

$$\frac{\partial \mathbf{u}}{\partial t} - P \frac{\partial \mathbf{u}}{\partial z} + Q\mathbf{u} = 0; \quad (4)$$

where $\mathbf{u}(z;t) = (v_r; v_\theta; b_r; b_\theta)^T$,

$$P = \begin{pmatrix} 0 & 0 & -\frac{\rho}{\rho_0} & 0 \\ 0 & 0 & 0 & -\frac{\rho}{\rho_0} \\ 1 & 0 & 0 & 0 \\ 0 & 1 & 0 & 0 \end{pmatrix}; \quad Q = \begin{pmatrix} 0 & 2 & 0 & 0 \\ \frac{1}{2} & 0 & 0 & 0 \\ 0 & 0 & 0 & 0 \\ 0 & 0 & \frac{3}{2} & 0 \end{pmatrix}; \quad (5)$$

where $\rho_0(z)$ is the steady state density profile, and $v_r; v_\theta; b_r$, and b_θ are the perturbed radial and azimuthal velocities ($v_r; v_\theta$), and the radial and azimuthal components of the magnetic field ($b_r; b_\theta$), respectively. In eq. (4) the density is normalized to its value at the disk midplane $\rho_0 = \rho(z=0)$, the velocities are normalized to $\sqrt{2}c_s$ (c_s is the sound velocity), the time is normalized to the inverse steady state angular velocity Ω^{-1} , the magnetic field is scaled with the steady state axial magnetic field B_z . Finally, lengths are scaled by $\sqrt{2}V_A$ where $V_A = B_z / \sqrt{4\rho_0}$ is the Alfvén velocity and Ω is the familiar plasma parameter given by $\Omega = 2c_s^2/V_A^2$.

As a specific example consider a thin isothermal Keplerian disk. In order to model the finite thickness of the disk the following profile

$$\rho(r;z) = \rho_0(r) \exp(-\frac{z^2}{2})$$

is assumed for the density. Due to the independence of the perturbations on the radial direction r is from now on merely a parameter. This is tantamount to the local approximation in r with $k_r = 0$, which according to Balbus & Hawley (1991) is the most unstable case. For that case, assuming that the IC are $\mathbf{u}(z;0) = (v_r(z;0); 0; 0; 0)$, and employing the Laplace transform, the set of eqs.(4) is reduced to the following single inhomogeneous ordinary differential equation (ODE):

$$L[\mathbf{B}] = 2i! \sqrt{2} V_A^0(z;0) \quad (6)$$

where

$$L[\mathbf{B}] = \frac{d}{dz} e^{z^2} \frac{d^2}{dz^2} e^{-z^2} \frac{\mathbf{B}}{dz} + (3 + 2\Omega^2) \frac{d}{dz} e^{z^2} \frac{\mathbf{B}}{dz} + \Omega^2 (z^2 \mathbf{B}); \quad (7)$$

$\omega = \omega_r - i\gamma$ represents the re-normalized spectral parameter ω , and \mathcal{B} is the Laplace transform of the azimuthal component of the perturbed magnetic field. The solution of eq.(6) should satisfy the following BC:

$$\mathcal{B}(1) = 0; \quad (\epsilon^2 \mathcal{B}^0)_{z=1}^0 = 2i \frac{\omega}{\omega_r} \mathcal{B}(1) - \epsilon^2 \mathcal{B}(1) = 0; \quad (8)$$

Boundary conditions (8) are obtained due to the requirement that at $z = 1$, where $\omega_r \neq 0$ and $B_z = \text{const}$, the energy flux of the perturbation is finite.

The solutions of the BVP (6)-(8) can be constructed by the countable set of the solutions of the homogeneous equation $L[\mathcal{B}] = 0$, subject to homogeneous boundary conditions. The solutions of that problem are termed eigenfunctions of the homogeneous equation. Assuming completeness and orthogonal property of the eigenfunctions allow to express the solution of eq.(6) in a simple way for an arbitrary IC by using Green's function (see appendixes A and B for proof of orthogonality, and construction of the Green's function). The latter is represented by an appropriate set of eigenfunction $\mathcal{B}_n(z)$. Thus, carrying out the inverse Laplace transform, the solution of eq.(4) for $t > 0$ is given by the following expression:

$$\mathcal{B}(z; t) = 4 \sum_n \frac{\mathcal{B}_n(z)}{\omega_n^2(z) - \omega_+^2(z)} \sin\left(\frac{\omega_+(z) - \omega_n(z)}{2} t\right) \sin\left(\frac{\omega_+(z) + \omega_n(z)}{2} t\right) \quad (9)$$

where $\mathcal{B}_n(z)$ are the eigenfunctions of the homogeneous equation, d_n are the coefficients of the expansion of $v_r^0(z; 0)$ in the complete set $\mathcal{B}_n(z)$, and $\omega_n(z)$ are the natural frequencies that correspond to the eigenfunctions $\mathcal{B}_n(z)$.

2.2 WKB solution

We turn now to obtaining asymptotic solutions for $\mathcal{B}_n(z)$ in the limit $\epsilon \ll 1$ [see (Erokhin & Moiseev 1973) as an example of employing the WKB approximation for some problems in inhomogeneous plasmas]. In that case the eigenfunctions may be represented by the following version of the WKB approximation:

$$\mathcal{B}_{jk} = e^{-z^2} S_k(z) = e^{-z^2} e^{S_k(z)}; \quad k = 1; \dots; 4; \quad (10)$$

Inserting expression (10) into the homogeneous part of eq.(6) yields:

$$S^{(4)} + \epsilon^2 [3P(z; \epsilon) S^{(2)} + 2Q(z; \epsilon) S^{(0)} + R(z; \epsilon)] + \frac{2S^{(2)} + S^{(0)}}{2} + 4S^{(0)} S^{(4)} + S^{(4)} = 0 \quad (11)$$

where

$$P(z; \epsilon) = \frac{1}{3} \frac{h}{\epsilon} e^{-z^2} (2 + 3\epsilon^2) \quad (6 + 4z^2)\epsilon^2; \quad Q(z; \epsilon) = \frac{h}{z} e^{-z^2} (2 + 3\epsilon^2) + 4\epsilon^2$$

and

$$R(z; \epsilon) = e^{-2z^2} (\epsilon^2 - 2\epsilon^2 z^2) - 2e^{-z^2} (2 + 3\epsilon^2);$$

By keeping the leading terms in ϵ , eq.(11) can be written as

$$S^{(4)} + \epsilon^2 [3P(z; \epsilon) S^{(2)} + 2Q(z; \epsilon) S^{(0)} + R(z; \epsilon)] = 0 \quad (12)$$

The solutions of eq.(12) provide valid approximations for the eigenfunctions of L throughout the disk except in the vicinity of the turning points. Assuming that the latter occur at $z_0 \approx 1$, it can be shown that the last term in eq.(12) becomes exponentially small in comparison with other terms (this assumption will be validated later on). In that case the equation that determines the turning points is given by

$$\frac{D(z_0; \epsilon)}{\epsilon} = \epsilon^2 P^3(z_0; \epsilon) + Q^2(z_0; \epsilon) = 0; \quad (13)$$

Asymptotic solution of eq.(13) for large ϵ yields the following expression for the turning points:

$$z_0 = \sqrt{\ln \frac{2}{\ln 2}} + O(\epsilon^{-3}); \quad (14)$$

as well as the following form of the discriminant in the vicinity of the turning points:

$$D(z; \epsilon) \approx K(z - z_0; \epsilon); \quad K = \frac{dD(z; \epsilon)}{dz} \Big|_{z=z_0} \approx 6\epsilon^2 (1 + 5z_0^2) \quad (15)$$

In the outer regions namely $z < z_0$ and $z > z_0$ all four functions $S_k(z)$ are real, whereas in the inner region $z_0 < z < z_0$ the solutions for $S_k(z)$ acquire non-zero imaginary part. Thus, the turning points separate the inner range $z_0 < z < z_0$ where the eigenfunctions are oscillatory from the outer regions $z < z_0$ and $z > z_0$ where the eigenfunctions decrease exponentially

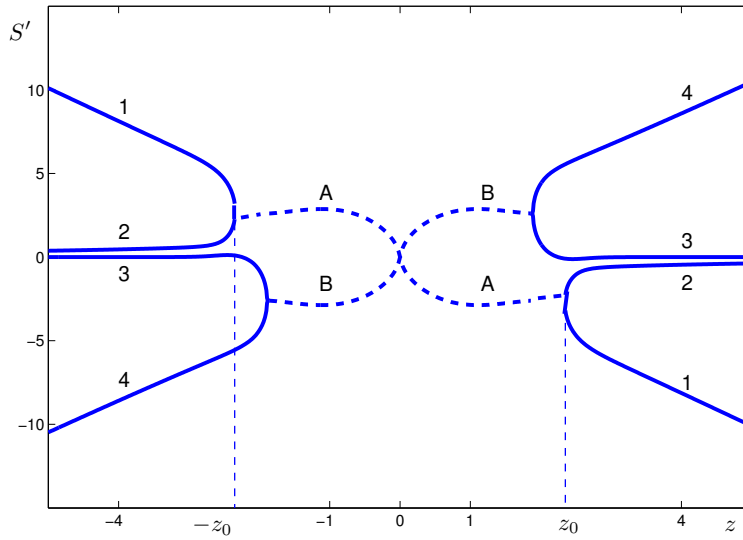


Figure 1. The solutions of eq.(12), obtained numerically for $\alpha = 10$; $\beta = 25$. Each of the dashed lines (A;B) represents the same real part of two complex conjugate solutions.

away from z_0 and have no zeros at a finite distance z . The behavior of the various solutions of eq.(12) as well as the turning points may be seen in Fig.1.

It is obvious from assumption (10) and BC (8) that only solution 1 is admissible. The turning points are obtained as the merging of solution 1 and 2. In the region between the turning points two solutions are admissible, that are complex conjugates of each other. Again, due to BC (8) those solutions are marked by A that depicts their common real part.

In the vicinity of the turning points the solutions assumed in eq.(10) are invalid and instead an appropriately re-scaled eq.(6) is solved. That solution is then matched asymptotically to the outer solution given by (10) and (12) where S^0 is obtained from branch 1 in Fig.1.

In order to obtain an asymptotic expression for S^0 in branch 1 it is noticed again that $R(z; \epsilon)$ is asymptotically much smaller than the rest of the terms that multiply ϵ in eq.(12). As a result, one of the roots is asymptotically zero (branch 3) while the rest three roots are obtained from the Cardano solution of the reduced eq.(12). Thus, the root that is represented by branch 1 (the only admissible root) gives rise to the following solution in the outer region close to the turning point:

$$(z) = \frac{C}{2^{1/4} \sqrt[4]{K} j(z-z_0)^{1/4}} \exp \left[\frac{Z}{z_0} \int_{z_0}^z \sqrt{K(z_0 - \xi)} d\xi \right] \quad (16)$$

In the inner region the solution near the turning points is given by

$$\frac{1}{\sqrt[4]{K} j(z_0 - z)^{1/4}} \left[C_1 \exp \left[i \frac{Z}{z_0} \int_{z_0}^z \sqrt{K(z_0 - \xi)} d\xi \right] + C_2 \exp \left[-i \frac{Z}{z_0} \int_{z_0}^z \sqrt{K(z_0 - \xi)} d\xi \right] \right] : \quad (17)$$

The coefficients ($C_{1,2}$) are determined by the connection formulas that express the asymptotic matching of the solution found to the left (17) and to the right (16) of a turning point z_0 . Following Landau & Lifshitz (1977) the connecting relations are:

$$C_{1,2} = \frac{C}{2} \exp \left(\pm \frac{i\pi}{4} \right):$$

Applying the same rule to the region close to the left turning point located at $-z_0$ and requiring that the two expressions are the same throughout the region $-z_0 < z < z_0$ (the sum of their phase must be multiple of π) results in the following expression for the eigenfunction:

$$\Psi_m(z; \epsilon) = \cos \left(\frac{h}{4} \right) \exp \left(\frac{i}{4} \right) e^{\frac{Z^2}{4}}; \quad (18)$$

where $(z) = \frac{R_{z_0}}{z} e^{\frac{Z^2}{2}}$. The analytical expression (18) for the solution in the inner region has been obtained by noticing that away from the turning points $S^0(z; \epsilon)$ is smaller than the rest of the terms in eq.(12) and hence to leading order the latter is a bi-quadratic equation. The discrete set of eigenvalues ϵ is now determined from the Bohr-Sommerfeld relation that is given by:

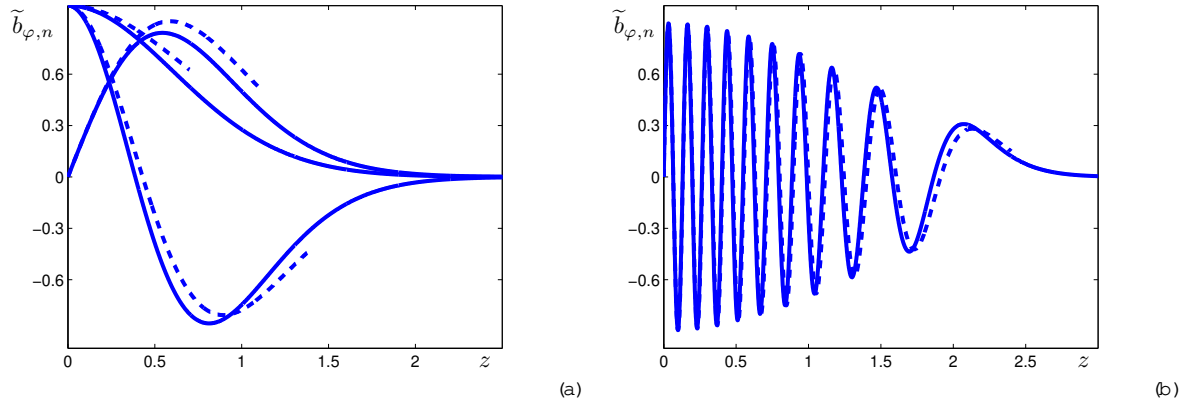


Figure 2. Comparison between the WKB solutions [eq.(18), dashed line] and the numerical solution (full line) of the homogeneous part of eq.(6); (a) for the first three eigenfunctions ($n = 0; 1; 2$) and (b) $n = 37$.

$$\tilde{b}_{\varphi,n} = \frac{r - q}{2} \frac{p}{3 + 2! (\omega_n)^2 + 9 + 16! (\omega_n)^2} = \frac{1}{(z_0)} n + \frac{1}{2} ; \quad (19)$$

The integer n in the last expression describes the number of zeros of the solution within the inner region [see eq.(18)], whereas ω_n are the natural frequencies of the system that correspond to such eigenfunctions. Strictly speaking expression (19) is valid for $n \gg 1$. Nevertheless, as is often the case for WKB-type solutions, numerical calculations indicate that expression (18) provides a close approximation also for n 's as low as 1 (see Fig 2). It is also evident from Fig 2 that the wave length of the perturbation depends on z and approaches the disk thickness close to the turning points.

As $n = 0$ is the first excited unstable mode, it is easy to show that the disk is stable for $\beta_0 < 6$ where $\beta_0 = (24 \text{Erf}(\frac{z_0}{2}))^2$ ($n = 1$; $\beta_0 = 3 = (8 \text{Erf}(\frac{z_0}{2}))^2$).

2.3 Numerical solution

To further follow the development of a localized initial perturbation governed by eq. (4), consider for example an IC given as:

$$v_r(z;0) = e^{-z^2/2}; \quad (20)$$

and zero for the rest of the initial values of the perturbed physical variables. It is easy to see that the perturbation is localized within the disk, if $\beta_0 < 1$. The dynamical development of the localized initial perturbation that is described by eq.(9) depends on the disk "thickness" defined by the plasma parameter β_0 (notice that now velocities are scaled by the Alfvén velocity which means that the disk thickness is $2\beta_0^{-1/2}$). If the disk is thin enough such that $\beta_0 < 6$ all the natural frequencies ω_n that are obtained from eq. (6) are real and hence the disk is stable. In that case following (9) the profile of the perturbed azimuthal magnetic field represented by two identical wave packets that move in opposite directions namely up and down. Upon reaching the upper and lower turning points (located at $\pm z_0$) the two packets are reflected and continue their motion through the disk. The amplitudes of the identical wave packets change in time like $1/\sin(t)$. It should be noted however that this picture is valid if the initial perturbation is localized enough. As an example for such behavior, $b_\varphi(z;t)$, which has been obtained by using eq.(9) $\omega_1 = 0.1$, and $\omega_3 = 3.99$ is depicted in Fig. 3. In this particular case all eigenfunctions have real natural frequencies [$\omega_1 = 1.54; 3.64; \omega_3 = 3.99; 6.01; \dots$] and there are no growing modes at all (the wave packets indeed do not grow in time, just move back and forth inside the disk with local Alfvén velocity).

For "thick" disk ($\beta_0 > 6$) some of the natural frequencies have an imaginary part. As the thickness of the disk increases so does the number of unstable modes. Thus for long time $b_\varphi(z;t) = \sum \tilde{b}_{\varphi,n}(z) \exp(j\omega_n t)$ where n corresponds to natural frequency with a biggest imaginary part. However, for sufficiently localized initial perturbation the fastest growing mode has sufficiently small initial amplitude. The perturbation then keeps its original shape for a long time until a growing mode emerges out of the wide initial spectrum and is of order of the amplitude of initial wave packet. Raising the value of β_0 to 10, one unstable mode, with growth rate $\gamma = 0.749$ enters the spectrum of the eigenmodes. Employing again eq.(9) together with eigenfunctions $\tilde{b}_{\varphi,n}(z)$ results in Fig 4. It is indeed seen that after long time the unstable mode dominates the perturbation. Thus, the latter event though starting as a well confined perturbation develops into a global instability. It should be noted however, that the time it takes the unstable mode to emerge from the wide spectrum that makes up the localized initial perturbation is about 4 times longer than the predicted growth time (inverse growth rate). Indeed, as the initial perturbation is more localized so the growth time of the most unstable mode is increased relative to its linear predicted value.

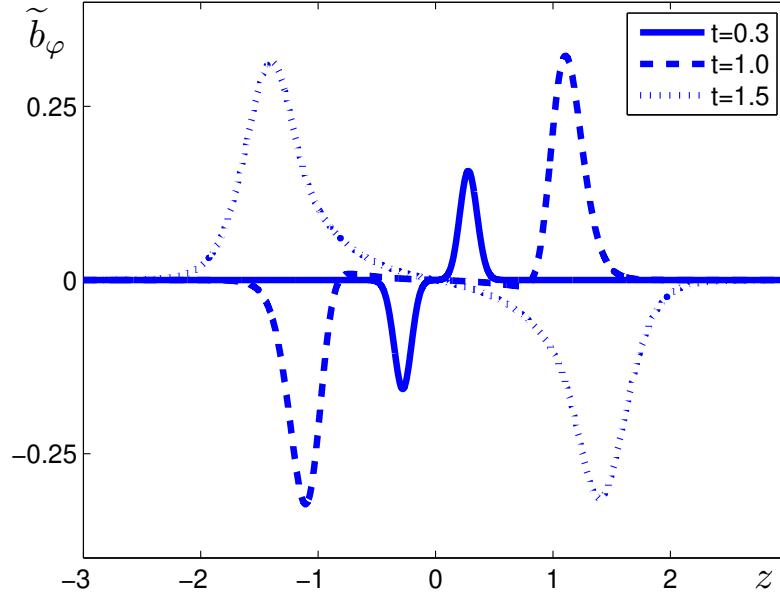


Figure 3. Time evolution of the profile of the perturbed azimuthal component of the magnetic field. The different profiles were calculated at times $[0.3, 1.0, 1.5]$ for $\beta = 3 = 8$, $\eta = 0.1$.

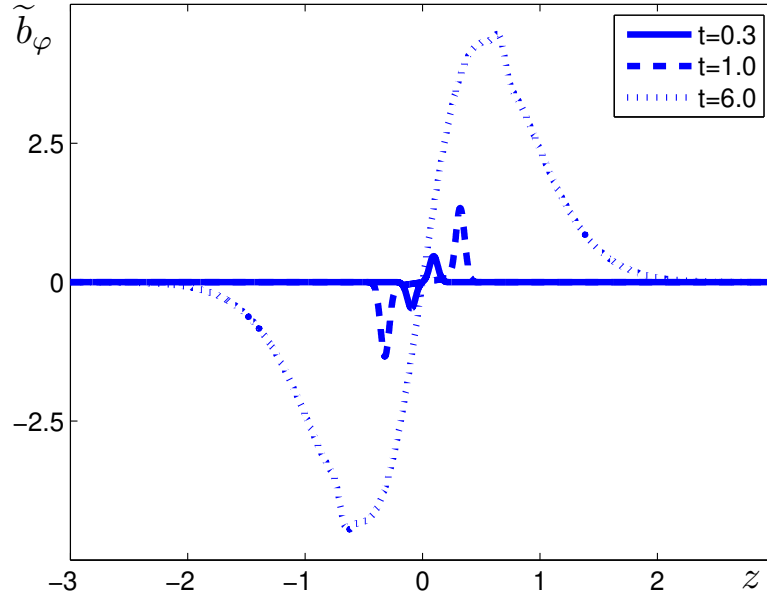


Figure 4. Long time evolution of the profile of the perturbed azimuthal component of the magnetic field for $\beta = 10$, $\eta = 0.05$. The different profiles were calculated at times $[0.3, 1.0, 6.0]$.

It is finally instructive to plot the wave number n of the most unstable mode as a function of β (Fig 5). A asymptotic estimation reveals that n is proportional to $\beta^{-1/2}$. This implies that the wavelength of the most unstable mode is of the order of $h = n^{-1} V_A = \lambda$ (where h is the thickness of the disk) which to leading order does not depend on η .

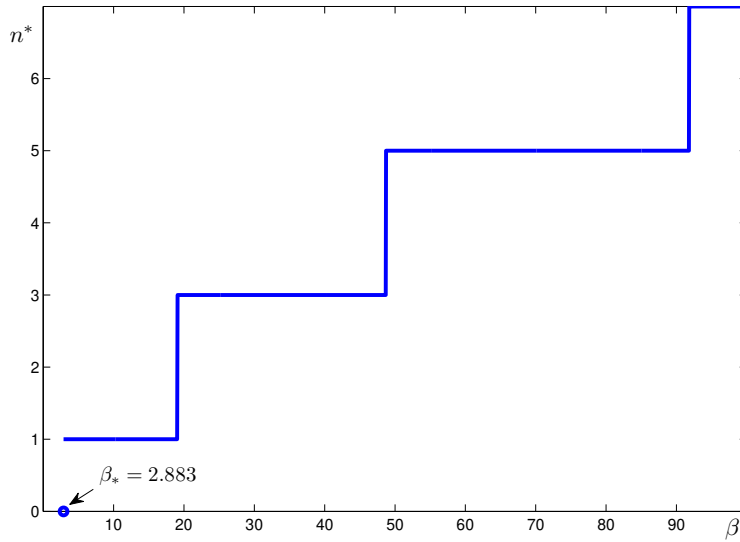


Figure 5. Axial standing wave number of the most unstable mode as a function of the plasma beta.

2.4 Limit of infinite "thickness"

It is instructive to examine the limit of thick disk such that effect of boundaries may be ignored. Such an assumption is justified when the Alfvén traverse time is longer than the time of interest (say inverse growth rate). Renormalizing therefore lengths to $V_A =$ solution is sought for $z = \frac{z}{2}$, where 2 is now the disk's thickness. It is readily seen that for such case $\mathcal{B}_m(z) \rightarrow \mathcal{B}(k; z) = \cos kz$ for odd initial perturbations [see eq.(18) where k is defined as $k = 2(n + 1/2)$] so that the eigenfunctions can be approximated by plane waves. Thus, due to $1 = \frac{1}{2} \rightarrow 0$, the sum (9) is replaced by an integral over k and eq.(9) can be written as

$$b(z; t) = \frac{1}{4\pi^2} \oint_C e^{i\omega t} d\omega \int_0^1 \frac{A(k) e^{ikz} dk}{D(k; \omega)} \quad (21)$$

where C is the contour of integration in the complex ω plane that is a straight line parallel to the real axis and passing above all singular points of the integrand, $A(k)$ is the Fourier transform of the right hand side of eq. (6) and the denominator of the integrand is given by

$$D(\omega; k) = (\omega^2 - k^2)^2 - \omega^2 - 3k^2 \quad (22)$$

It is important to notice now that since the initial perturbation is well localized in space $A(k)$ in contrast is close to a constant that is proportional to the localization length. As a result it can be shown now that $b(z; t)$ obtained by using (21) is not zero only if the integrand has a singularities of order two (branch points) (see in details in Fainberg et al. (1961); Akhiezer & Polovin (1971)). Thus, examining the equation $D(\omega; k) = 0$ [the classical MRI dispersion equation (Balbus & Hawley 1991)] it is clear that there is just one branch point that gives rise to instability, which is $\omega = 3i/4; k = \sqrt{15}/4$. Consequently, the long time behavior of the perturbation is given by

$$b(t) \sim e^{3t/4} = e^{\frac{3}{4}t} \quad (23)$$

As remarked above this result is due to the fact that the initial perturbation is localized in space. If, however, (a not too physical) monochromatic perturbation is considered, $A(k)$ is a delta function and the familiar purely exponential growth is recovered.

3 CONCLUSIONS

The importance of solving the initial value problem with some appropriate boundary conditions is highlighted. In the classical works of Velikhov (1959); Chandrasekhar (1960), and Balbus & Hawley (1991), an infinite cylinder has been considered and the effects of the boundary conditions were neglected. Therefore, in those works, naturally, the thickness of the disk does not play any role and consequently cannot influence the extent of the domains of instability. In spite of that, physical intuition and

insight have led Balbus & Hawley (1991) to conclude that l is the lower limit for the disk thickness for the occurrence of the classical MRI in disks as for smaller values of l the thickness of the disk is smaller than the wave length of the dominant unstable mode. In the current work the stabilizing effects of the boundaries are taken explicitly into account and hence the threshold thickness of the disk may be calculated easily from the WKB solutions obtained in Sec.2. Furthermore, the number of unstable modes as a function of l may be estimated with the aid of that solution. Thus, for example, it may be shown that there are only three unstable modes within the disk as long as the β value is less than 15. Such information is significant for the study of the consequent nonlinear development of the instability. In addition, the shape of the unstable (as well as the stable) perturbations has been obtained explicitly and as may be seen by its expression (18) may differ significantly from the plain waves assumed in the classical works on MRI's. It is finally interesting to note, that going to the limit of thick disks (see Section 2.4) and assuming a localized perturbation results in a reduced rate of growth in comparison to the less realistic monochromatic classical result [see Eq.(23)]. Recently, Coppi & Coppi (2001), and Coppi & Keyes (2003) have considered the effects of the axial localization of the perturbations by studying axisymmetric ballooning modes in finite disks. Such modes are characterized by finite values of the radial wave vector k_r . The appropriate turning points within the disk were found and consequently a discrete spectrum of eigenfunctions and eigenvalues was obtained. The growth rates were found to be smaller than their "long-cylinder" counterparts. In particular, it is shown there that the $k_r \rightarrow 0$ limit cannot be obtained from their scalings and asymptotics, as no turning points exist within the disk in that limit. In that sense the present work is complementary to (Coppi & Keyes 2003) as it analyzes that very limit $k_r \rightarrow 0$. Indeed, under the current scaling and asymptotic expansion turning points are found within the disk and the corresponding discrete spectrum is obtained.

The linear MHD equations have been employed in order to study the stability and time behavior of a rotating stratified Keplerian disks whose density decreases with height. The full solution of the dynamical evolution in time of an localized Gaussian wave packet is explicitly derived and its long time behavior is discussed. It is proven analytically (WKB) that MRI can be suppressed in sufficiently thin disk $l < l_{crit} = 11$ Miller & Stone (2000) observed from numerical simulations that if

$l > l_{crit}$ the disk becomes MRI stable). Numerical solutions of the Cauchy problem however, indicates that l_{crit} is of order 1. This result is consistent with values obtained by Sano & Miyama (1999). For thicker disks, the number of discrete unstable mode increases with the thickness of the disk. However, due to the localization in real space the initial amplitude of the unstable mode is diminishingly small and the time it outgrows the original wave packet is significantly longer than its predicted inverse growth rate. Thus, it has been demonstrated numerically the growth time of a perturbation that is initially localized within the inner 5% of the disk, may be an order of magnitude longer than the inverse growth rate of the fastest growing unstable mode.

The considering of the boundary effects may have a large impact on the design of laboratory experiments to model MRI, where a magnetic field have to be quite strong and devices cannot be very high.

ACKNOWLEDGMENTS

The authors are greatly indebted to Oded Regev and Orkan Umurhan for fruitful discussions and insights, as well as for their encouragement.

REFERENCES

- Akhiezer, A.I., Polovin, R.V. 1971, *Usp Fiz Nauk*, 104, 185 [1971, *Soviet Physics Uspekhi*, 104, 278]
- Balbus, S.A., Hawley, J.F., 1991, *ApJ*, 376, 214
- Budker, G.I., 1956, *Atomic Energy*, 1, issue 5, 673
- Chandrasekhar, S. 1960, *Proc. Nat. Acad. Sci.*, A 46, 223
- Coppi, B., Coppi, P.S., 2001, *Phys. Rev. Lett.*, 87, 051101
- Coppi, B.; Keyes, E.A., 2003, *ApJ*, 595, 1000
- Drazin, P.G. 2002, *Introduction to Hydrodynamic Stability*, (Cambridge: University Press)
- Erokhin, N.S., Moiseev, S.S. 1973, *Voprosy teorii plazmy*, v.7, p.146 (Moscow: Atomizdat, 1973) [Reviews of plasma physics, Edited by A.I. Leontovich, v.7, 181, (New York: Consultants Bureau, 1979)]
- Fainberg, Ya.B., Kuriklo, V.I., & Shapiro, V.D. 1961, *Zhurnal Tekhnicheskoi Fiziki*, 31, 633 [1961, *Soviet Physics-Technical Physics*, 6, 459].
- Gallitis, A., Lielakis, O., Platadis, E., Gerbeth, G., & Stefani, F. 2004, *Phys. Plasmas*, 11, 2838
- Huerre, P., Monkevit, P.A. 1990, *Annu. Rev. Fluid Mech.*, 22, 473
- Ji, H.T., Burin, M., Scharfman, E., & Goodman, J. 2006, *Nat.*, 444, 343
- Landau, L.D., 1946, *Zh. Eksp. Teor. Fiz.*, 16, 574 [1946, *J. Phys. USSR*, 10, 25]
- Landau, L.D., Lifshitz, E.M. 1959, *Fluid Mechanics*, (Oxford: Pergamon Press)
- Landau, L.D., Lifshitz, E.M. 1977, *Quantum mechanics: non-relativistic theory*, (Oxford: Pergamon Press)

- Lifshitz, E.M., Pitaevskii, L.P. 1981, Physical kinetics, (Oxford: Pergamon Press)
- Miller & Stone, 2000, ApJ, 534, 398
- Noguchi, K., Pariev, V.I., Colgate, S.A., Beckley, H.F., & Nordhaus, J. 2002, ApJ, 575, 1151
- Rudiger, G., Hollerbach, R., Stefani, F., Gundrum, T., Gerbeth, G., & Rosner, R. 2006, ApJ, 649, L145
- Sano T., Miyama S.M., 1999, ApJ, 515, 776
- Sturrock, P.A. 1958, PhysRev.A, 112, 1488
- Velikhov, E.P. 1959, Zh. Eksp. Teor. Fiz., 36, 1398 [1959, Sov.Phys. JETP, 9,995]

APPENDIX A: ORTHOGONALITY

Both sides of the homogeneous equation $L[\Psi_m(z)] = 0$ are first multiplied by $\Psi_m(z)$ and then integrated over the interval $(-1; 1)$. Integrating by parts and setting the boundary terms to zero due to the homogeneous BC (6) yields

$$\int_{-1}^1 \Psi_m e^{z^2} e^{z^2} \Psi_m^0 dz + 3 \int_{-1}^1 e^{z^2} \Psi_m^0 dz + 2 \int_{-1}^1 \Psi_m e^{z^2} \Psi_m^0 dz + \frac{2}{n} \left(\frac{2}{n} \right) \int_{-1}^1 \Psi_m \Psi_m dz = 0 \quad (A1)$$

Dening

$$Q_{1m,m} = \int_{-1}^1 \Psi_m \Psi_m dz; \quad Q_{2m,m} = \int_{-1}^1 \Psi_m e^{z^2} \Psi_m^0 dz = \int_{-1}^1 \Psi_m e^{z^2} \Psi_m^0 dz;$$

and noticing that to each eigenfunction Ψ_m correspond two eigenvalues $\frac{2}{n;1;2}$ allows rewriting (A1) in the form of the following set of homogeneous linear equations:

$$AQ = 0; \quad Q = (Q_{1m,m}; Q_{2m,m})^T; \quad A = \begin{pmatrix} \frac{2}{n;1} \left(\frac{2}{n;1} \right) & \frac{2}{m} \left(\frac{2}{m} \right) \\ \frac{2}{n;2} \left(\frac{2}{n;2} \right) & \frac{2}{m} \left(\frac{2}{m} \right) \end{pmatrix} \quad (A2)$$

Implying that different eigenfunctions ($n \neq m$) have different eigenvalues results in:

$$\det(A) = 2 \left(\frac{2}{n;1} \right) \left(\frac{2}{n;2} \right) \left(\frac{2}{n;1} \right) \left(\frac{2}{m} \right) \left(\frac{2}{n;2} \right) \left(\frac{2}{m} \right) \neq 0: \quad (A3)$$

This implies that

$$Q_{1m,m} = Q_{2m,m} = 0: \quad (A4)$$

In the opposite case of identical eigenfunctions ($m = n$) the equality $\det(A) = 0$ means that $Q_{1m,m} \neq 0$. Combining the latter with eq.(A4) gives

$$\int_{-1}^1 \Psi_m \Psi_m dz = k \int_{-1}^1 \Psi_m \Psi_m^0 dz = k \int_{-1}^1 \Psi_m^2 dz: \quad (A5)$$

APPENDIX B: GREEN'S FUNCTION

To obtain the expansion coefficients c_n of a solution $\Psi_p(z)$ for the inhomogeneous equation $L[\Psi_p(z)] = f(z)$ in terms of the eigenfunctions $\Psi_m(z)$ the solution expansion $\Psi_p(z) = \sum_1 c_1 \Psi_{;1}(z)$ and expansion of the r.h.s of the inhomogeneous equation $f(z) = \sum_m d_m \Psi_m(z)$ is substituted into the inhomogeneous equation. The result is multiplied by $\Psi_m(z)$ and integrated over the interval $(-1; 1)$. The result is

$$\sum_1 c_1 \int_{-1}^1 \Psi_m L[\Psi_{;1}] = \sum_m d_m \int_{-1}^1 \Psi_m \Psi_m^0 dz: \quad (B1)$$

Dening in addition to $Q_{1m;1}$ and $Q_{2m;1}$

$$Q_{3m;1} = \int_{-1}^1 \Psi_m e^{z^2} e^{z^2} \Psi_{;1}^0 dz;$$

and employing the homogeneous equation $L[\Psi_{;1}] = 0$ multiplied by $\Psi_m(z)$ and integrated over the interval $(-1; 1)$ yields:

$$Q_{1m;1} = k \int_{-1}^1 \Psi_{;1}^2 dz; \quad Q_{2m;1} = \frac{k \int_{-1}^1 \Psi_{;1}^2 dz}{2} \left(\frac{2}{l;1} + \frac{2}{l;2} \right) n;1; \quad Q_{3m;1} = \frac{k \int_{-1}^1 \Psi_{;1}^2 dz}{2} \left(3 \left(\frac{2}{l;1} \right) + \frac{2}{l;2} \left(2 \frac{2}{l;1} + 3 \right) \right) n;1: \quad (B2)$$

Thus eq.(B1) can be rewritten as

$$c_n \left(\frac{2}{n;1} \right) \left(\frac{2}{n;2} \right) = d_n; \quad (B3)$$

and a solution of the inhomogeneous equation with r.h.s $f(z)$ has a form :

$$\mathfrak{S}(z) = \sum_n \frac{d_n \mathfrak{S}_n(z)}{(\frac{z^2}{n+1} - 2)(\frac{z^2}{n+2} - 2)} : \quad (\text{B } 4)$$

Finally noticing that $d_n = \frac{1}{k \mathfrak{S}_n k^2} \int_{-1}^1 f(z) \mathfrak{S}_n(z) dz$, a solution of inhomogeneous equation (B 4) can be rewritten as

$$\mathfrak{S}(z) = \int_{-1}^1 G(z; \zeta) f(\zeta) d\zeta ; \quad (\text{B } 5)$$

where

$$G(z; \zeta) = \sum_n \frac{\mathfrak{S}_n(z) \mathfrak{S}_n(\zeta)}{(\frac{z^2}{n+1} - 2)(\frac{\zeta^2}{n+2} - 2) k \mathfrak{S}_n k^2}$$

is a Green's function written in terms of an eigenfunctions $\mathfrak{S}_n(z)$.

This paper has been typeset from a $\text{T}_{\text{E}}\text{X}$ / \LaTeX file prepared by the author.